Atomistic Monte Carlo Simulation of Polybutadiene Isomers: *cis*-1,4-Polybutadiene and 1,2-Polybutadiene

P. Gestoso,[†] E. Nicol,[†] M. Doxastakis,[†] and D. N. Theodorou*[,†,‡]

Institute of Chemical Engineering and Temperature Chemical Processes, P.O. Box 1414, 26500 Patras, Greece, and School of Chemical Engineering, Department of Materials Science and Engineering, National Technical University of Athens, 9 Heroon Polytechniou Street, Zografou Campus, 15780 Athens, Greece

Received January 9, 2003; Revised Manuscript Received June 30, 2003

ABSTRACT: Atomistic simulations of two isomers of polybutadiene (PB), *cis*-1,4-PB and 1,2-PB, have been conducted using the end-bridging Monte Carlo algorithm. The maximum mean molecular lengths of the polymer chains were C_{1000} and C_{161} for *cis*-1,4-PB and 1,2-PB, respectively. The simulated ensembles of configurations were evaluated in terms of equilibration rate and conformational, volumetric, and structural properties. The results illustrate the correlation between successful end-bridging, reptation, and concerted rotation (CONROT) moves and the enhanced equilibration rate of large systems with long chains. Comparison with experimental data shows that the simulations underestimate the specific volume to some extent, especially for 1,2-PB. Simulation predictions for the torsion angle distribution, end-to-end distance, radius of gyration, and characteristic ratio are in good agreement with experiment, confirming the ability of the force field to reproduce the structure of real PB melts. Analysis of geometric features of the pure component intermolecular pair distribution functions is applied to gain insight about miscibility in polybutadiene/polyisoprene binary blends.

Introduction

Polybutadienes play a very important role in rubber technology. The economic stakes linked to these materials have encouraged extensive experimental research efforts. Today, the progress accomplished in the area of polymerization allows satisfactory control of molar masses and microstructures. The wealth of data available for polybutadiene with different microstructures (1,4 and 1,2) and configurations (*cis*-1,4 and *trans*-1,4) make it attractive for theoretical modeling and simulations. Mark[1] studied the random coil configuration of *cis*-1,4-PB and *cis*-1,4-polyisoprene (*cis*-1,4-PI) using the rotational isomeric state (RIS) model. These calculations were extended by Abe and Flory,[2] introducing trans units and exploring the effect of stereoirregularity. More recently, Ma and Zhang[3] calculated the unperturbed mean-square radius of gyration of 1,2-PB, also called poly(vinylethylene) (PVE), using the RIS theory. Mattice and co-workers[4,5] have studied the properties of PB extensively, using molecular mechanics (MM) and molecular dynamics (MD). They investigated the thermodynamic and conformational properties, but also the static free volume.[6] Gee and Boyd[7] have studied the conformational dynamics and the relaxations in bulk PB using MD simulation. Recently, Smith et al.[8] have developed a new united atom force field for the simulation of 1,4-PB, based on quantum chemistry calculations. They conducted MD simulations of molten 1,4-PB and compared the local and chain dynamics with ^{13}C NMR and neutron spin-echo experiments.[9]

The MD technique is limited to short chain systems (up to 1350 g mol^{-1} for 1,4-PB[8,9]), and the accessible simulation time scales are under 200 ns. On the other hand, Monte Carlo (MC) simulations are known to be very efficient in equilibrating structures composed of long polymer chains with the aim of obtaining the structural and thermodynamic properties of these systems. The use of efficient moves, such as configurational-bias (CB),[10−14] concerted rotation (CONROT),[15,16] and end-bridging (EB),[16,17] has allowed a relatively fast equilibration of long chains by atomistic MC. Recently, the EB move has been successfully used to simulate linear polyethylene (PE) melts consisting of 6000 carbon long chains (number-average molar mass $\bar{M}_n = 84\,000$ g mol^{-1}).[18] Atomistic MC has also been extended to more complex polymers, such as polypropylene (PP)[19,20] and *cis*-1,4-PI.[21]

In this work we present atomistic MC simulations of two polybutadiene isomers: *cis*-1,4-polybutadiene (*cis*-1,4-PB) and 1,2-polybutadiene (1,2-PB). To accelerate equilibration of the model systems, a mix of five moves is implemented: end-bridging, concerted rotation, configurational-bias reptation, rotation of chain ends, and volume fluctuation. Conformational, volumetric, and thermodynamic properties of the simulated melts are calculated and compared to experimental data in order to evaluate the ability of the models to predict physical properties. Finally, an analysis of the pair distribution functions for the pure components is used to gain insight about the miscibility behavior of blends of the polybutadienes with polyisoprene.

Molecular Model

As in the previous work on *cis*-1,4-PI,[21] we used a united atom model in which every CH_n group in the chain is represented by a single interaction site (Figure 1). The bond lengths and bond angles are kept constant during the simulation. Their values have been taken from ref 8 and are reported in Table 1. The potential energy associated with the dihedral angles was calcu-

[†] Institute of Chemical Engineering and Temperature Chemical Processes.
[‡] National Technical University of Athens.
* To whom correspondence should be addressed at NTU Athens: Tel +30210 772 3157; Fax +30210 772 3112; e-mail doros@central.ntua.gr.

10.1021/ma034033l CCC: $25.00
Published on Web 08/12/2003

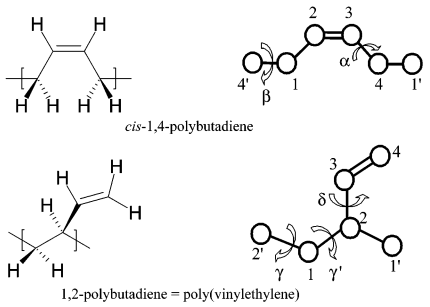

Figure 1. United atom model for *cis*-1,4-polybutadiene (top) and 1,2-polybutadiene (bottom). Atom numbering is used to describe the bond length and the bond angle values given in Table 1.

Table 1. Geometric Parameters Used for *cis*-1,4-PB and 1,2-PB

	bond lengths l (Å)		bond angles θ (deg)	
cis-1,4-PB	1−2	1.51	123	125
	2−3	1.34		
	3−4	1.51	341′	112
	4−1′	1.53		
1,2-PB	1−2	1.53	121′	111.65
	2−3	1.51	123	111.65
	3−4	1.34	234	125.89
	2−1′	1.53		

lated using the torsional potential developed previously by Smith and Paul:[8,9]

$$E_\phi = \frac{1}{2}\sum_{n=1}^{6} k_n(1 - \cos(n\phi)) \qquad (1)$$

The set of parameters k_n ($n = 1, ..., 6$) corresponding to torsions of dihedral angles α and β for *cis*-1,4-PB and γ, γ' and δ for 1,2-PB (see Figure 1) are reported in Table 2. For *cis*-1,4-PB, the dihedral angle associated with the double bond is kept constant to the value 0°. For 1,2-PB, the torsional energies associated with the δ angles in the two directions of the chain were calculated, and their average was added to the total energy function. This accounts for the fact that the dihedral angle associated with the vinyl group is different according to the direction in which it is calculated.

All nonbonded interactions, the intermolecular as well as the intramolecular (atoms separated by more than three bonds), were calculated using a Lennard-Jones potential (eq 2) with a cutoff distance set at $R_{cutoff} = 2.5\sigma$ for *cis*-1,4-PB and $R_{cutoff} = 2.3\sigma$ for 1,2-PB, with $\sigma = (r_{min}/2^{1/6})$. Tail corrections are fully taken into account by direct integration. It is important to point out that ongoing MC simulations using a $R_{cutoff} = 2.3\sigma$ for *cis*-1,4-PB show no substantial differences from the results presented in this paper in terms of structure [as measured by the intrachain pair density function $w(r)$ and the intermolecular pair distribution function $g(r)$] and thermodynamic properties. The values of the constants r_{min} and ϵ are taken from ref 8 and are reported in Table 3, along with the values of R_{cutoff} for both isomers.

$$U_{LJ} = \epsilon\left[\left(\frac{r_{min}}{r}\right)^{12} - 2\left(\frac{r_{min}}{r}\right)^{6}\right] \qquad (2)$$

1,2-PB chains are atactic, containing 50% meso dyads. Each atactic chain is considered as a Bernoullian sequence of meso and racemo dyads, with the probability (frequency) of meso dyads being $w_m = 0.50$. This is a typical assumption for vinyl polymers and has already been invoked (with $w_m = 0.48$) in modeling equilibrium epimerized atactic polypropylene,[19,20,22] whose stereochemical configuration has been fully characterized experimentally. No analogous stereochemical characterization is available for 1,2-PB; Bernoullian sequences with 50% meso dyads are postulated as the simplest stereochemical configuration that would be consistent with the synthetic procedure whereby the polymer is obtained.

Simulation Method

The end-bridging Monte Carlo method was implemented to simulate *cis*-1,4-PB and 1,2-PB. Previous works have shown the efficiency of this method for the simulation of long-chain polymer systems[17,18] due to an enhanced sampling of configuration space. The method was used in the semi-grand canonical ensemble $NnPT\mu^*$, where the number of chains (N), the number of mers (n), the temperature (T), the pressure (P), and a profile of relative chemical potentials (μ^*) are kept constant.

A mix of the five following moves was used to equilibrate the structures: chain-end rotation (10%), configurational-bias reptation (CB) (25%), concerted rotation (CONROT) (39.5%), end-bridging (EB) (25%), and volume fluctuation (0.5%). The percentages have been chosen in preliminary runs in order to improve the rate of system equilibration.

As in the case of *cis*-1,4-PI, the double bond in the *cis*-1,4-PB constrains the four atoms of a monomer to lie in the same plane. We have used the same kind of mapping[21] to build a hypothetical central atom of the repeat unit (see Figure 4 of ref 21). This construction allows us to apply the Monte Carlo moves previously developed for PE and for PI.

The design of the chains used to simulate 1,2-PB is not strictly a replication of 1,2-butadiene repeat units. We add a terminal united atom 1 (Figure 1) at the end of each chain in order to introduce a symmetric chemical structure. This improves efficiency, particularly for the end-bridging move.

Chain-End Rotation. This move induces a random rotation of a monomer at the beginning or the end of a chain. For *cis*-1,4-PB the procedure was analogous to that previously described for *cis*-1,4-PI:[21] The torsion angle changes are picked in a continuous interval (−60°,+60°).

In the case of 1,2-PB, a first rotation is made around the last atom 1−atom 2 bond (see Figure 1). Atoms 3 and 1′ are rebuilt. A second rotation around the atom 2−atom 3 bond is then used to place atom 4 of the vinyl group. Again, the torsion angle changes are picked in a (−60°,+60°) interval.

Volume Fluctuation. This move allows sampling fluctuations of the system density. It is conducted as for PE.[17]

Concerted Rotation (CONROT). This move is implemented in order to introduce local conformational rearrangements inside the chains. It can be compared to a "crankshaft" motion of a chain segment. For *cis*-1,4-PB, this move is performed in the same way as for *cis*-1,4-PI,[21] employing the same kind of mapping. For 1,2-PB, we proceed as for PE[15,16] for the intramolecular rebridging in the main chain. Then atom 3 (see Figure 1) is rebuilt, after introducing a random selection of the

Table 2. Parameters Used for the Torsional Potential (k_n in kcal/mol)

	torsion	k_1	k_2	k_3	k_4	k_5	k_6
cis-1,4-PB[a]	α	1.033	−0.472	0.554	0.263	0.346	0.164
	β	−0.888	−0.619	−3.639	−0.066	−0.247	−0.190
1,2-PB[b]	γ, γ'	−2.60	−1.05	−2.27	−0.28	−0.12	−0.26
	δ	−1.52	0.72	0.75	−0.15	0.11	−0.09

[a] From ref 8. [b] From ref 9.

Table 3. Lennard-Jones Parameters Used for the Nonbonded Pair Interactions

				R_{cutoff} (Å)	
i	*j*	ϵ_{ij} (kcal/mol)	r_{min} (Å)	*cis*-1,4-PB	1,2-PB
CH_2	CH_2	0.0936	4.500	10.023	9.221
CH_2	CH	0.1015	4.257		8.723
CH_2	CH=	0.1015	4.257	9.481	8.723
CH_2	CH_2=	0.1015	4.257		8.723
CH	CH	0.1000	3.800		7.786
CH	CH=	0.1000	3.800		7.786
CH	CH_2=	0.1000	3.800		7.786
CH=	CH=	0.1000	3.800	8.464	7.786
CH=	CH_2=	0.1000	3.800		7.786
CH_2=	CH_2=	0.1000	3.800		7.786

chirality in order to maintain the atacticity of the chains. We build atom 4 of the vinyl group by selecting a torsion angle change around the atom 2−atom 3 bond in a continuous interval (−60°,+60°).

The question of changing the chirality in atactic polymers with a Bernoullian distribution of dyads through CONROT and EB MC moves has been considered in detail by Samara.[19,20] In Samara's work, the semigrand ensemble sampled by the EBMC method was generalized to allow variations in the stereochemical sequences of the chains. Moves switching the chirality of pseudoasymmetric skeletal atoms were introduced, and their acceptance probability was shown to incorporate an additional factor, equal to the ratio of the product of probabilities for the newly created dyads to the product of probabilities of the eliminated dyads. In this ratio, meso dyads are assigned a probability w_m and racemo dyads a probability $1 - w_m$. In all atactic 1,2-PB systems simulated here, w_m was taken equal to 0.5; hence this ratio reduces to unity. That the statistics of the distribution of stereochemical sequences remains Bernoullian with $w_m = 0.5$ throughout the simulation runs was checked by direct accumulation of the frequencies of all types of dyads and triads in the melt, following Samara's analysis for atactic PP.[19]

Configurational-Bias Reptation (CB). The reptation move is performed in a biased way, which avoids overlaps with intramolecular or intermolecular neighbors.[10−14] A monomer unit is removed at the beginning or the end of a chain and is rebuilt, atom by atom, at the other extremity of the same chain. First, 10 trial positions are randomly chosen for each atom to be rebuilt. Then, one set of positions is selected according to the Boltzmann statistical weight of all the trial sets. For *cis*-1,4-PB, the position of atom 4 is calculated from the positions of atoms 2 and 3. In the case of 1,2-PB, a new chirality is randomly chosen for atom 2, and the position of atom 3 is calculated from the positions of atoms 2 and 1′. Finally, the appropriate acceptance criterion is applied in order to remove the bias introduced by the selection process.

End-Bridging (EB). This move has already been used extensively for PE[17,18] and PI.[21] It is known to enhance the equilibration of long chain systems and to introduce polydispersity. The strategy applied in the case of *cis*-1,4-PB emulates that used for *cis*-1,4-PI.[21] Unlike for *cis*-1,4-PI, a chain end of *cis*-1,4-PB is allowed to bridge in both directions of the target chain because of the higher symmetry of the *cis*-1,4-PB chain (see Figure 2). This increases the number of potential bridgeable neighbors by a factor of 2.

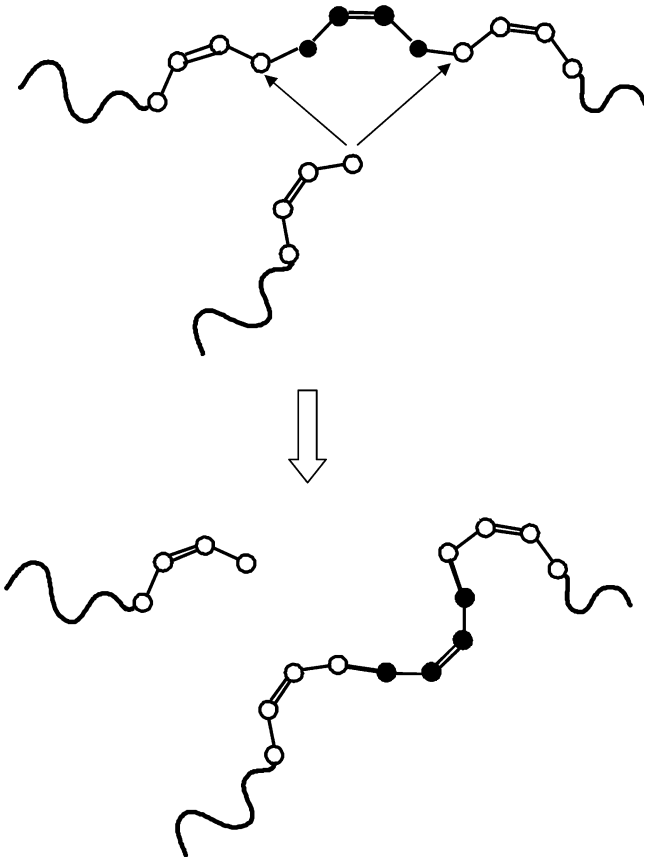

Figure 2. Schematic representation of the end-bridging move for *cis*-1,4-PB. Because of the symmetry of the model, the end-bridging move is allowed to occur in both directions of the chain. Details concerning the procedure used have been described in ref 21.

For 1,2-PB, the procedure is based on the end-bridging method used for PE. This move is illustrated in Figure 3. (a) A chain end is randomly selected to attack a target atom of a different chain selected from the neighbor list. Because of the symmetry of the 1,2-PB chains, this end is also allowed to bridge in both directions of the target chain. (b) The geometric problems are solved in the same way as for PE, and each atom 3 (in the numbering scheme of Figure 1) is rebuilt by selecting randomly a new chirality. One prospective solution for the bridge is chosen according to the Boltzmann statistical weight of the trial positions. (c) Each atom 4 is then rebuilt separately in a biased way in order to increase the acceptance ratio of the end-bridging move, using the same method as for CB reptation. The total acceptance criterion involves a product of three acceptance probabilities (P_{bridge} for the

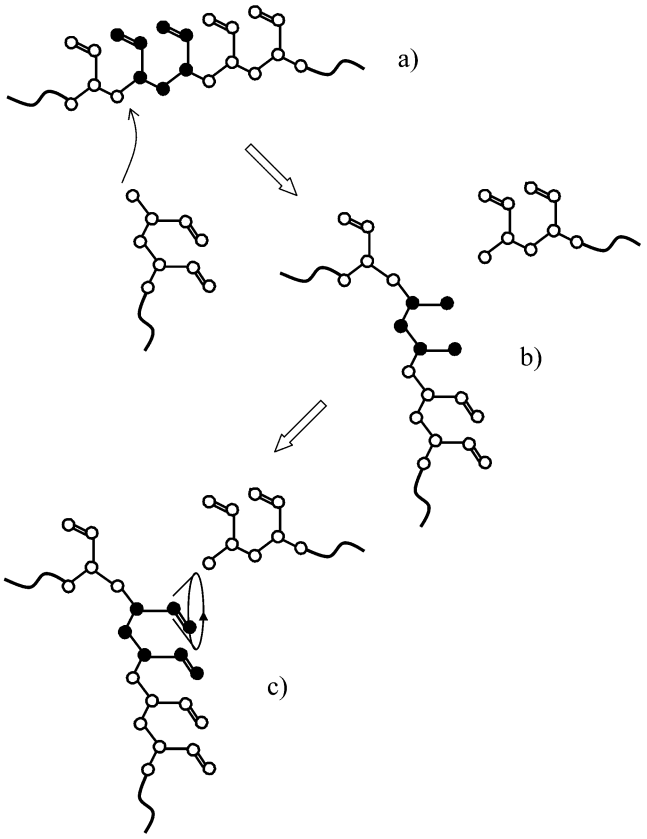

Figure 3. Schematic representation of the end-bridging move for 1,2-PB: (a) A chain end attacks a backbone atom on a different chain. (b) The backbone atoms are rebuilt in the same fashion as for PE. Atoms 3 are rebuilt by selecting randomly a new chirality. (c) Each atom 4 is then rebuilt separately in a biased way.

end-bridging, P_{bias1} for the first atom 4, and P_{bias2} for the second atom 4):

$$P_{\text{EB}} = \min[1, P_{\text{bridge}} \times P_{\text{bias1}} \times P_{\text{bias2}}] \qquad (3)$$

The acceptance criterion P_{bridge} is described in ref 16, and the acceptance criteria for the bias moves (P_{bias1} and P_{bias2}) are described in ref 10.

Systems Studied

As discussed in the "Simulation Method" section, our *cis*-1,4-PB melts consist of chains of the type $C_XH_{3X/2+2}$ with X being a multiple of 4. Our 1,2-PB melts consist of chains of the type $C_XH_{3X/2+5/2}$ with $X - 1$ being a multiple of 4. We will use the number of carbon atoms X as a measure of chain length in the following. We have studied *cis*-1,4-PB melts of various average molar masses (from 434 to 13 502 g mol^{-1}) at different temperatures (from 343 to 413 K) and at a pressure of 1 atm. For a mean chain length $\bar{X}$, the number distribution of chain lengths is uniform in the interval $[\bar{X}(1 - \Delta), \bar{X}(1 + \Delta)]$. The polydispersity index of each melt is calculated by the following equation: $I_p = 1 + \Delta^2/3$, where Δ represents the half-width of the chain length distribution reduced by the number-average chain length. Systems up to 3242 g mol^{-1} (C_{240}) were simulated with $\Delta = 0.5$ ($I_p \approx 1.08$), while a value of $\Delta = 0.4$ ($I_p \approx 1.05$) was selected for the longest chain systems (C_{400} to C_{1000}). The system parameters for all melts are reported in Table 4.

Table 4. System Parameters for *cis*-1,4-PB and 1,2-PB Melts

		no. of chains	total no. of atoms	M (g mol^{-1})
cis-1,4-PB	C_{32}	168	5376	434
	C_{48}	80	3840	650
	C_{64}	64	4096	866
	C_{96}	40	3840	1298
	C_{128}	32	4096	1730
	C_{240}	32	7680	3242
	C_{400}	32	12800	5402
	C_{600}	24	14400	8102
	C_{1000}	24	24000	13502
1,2-PB	C_{33}	160	5280	448
	C_{49}	80	3920	664
	C_{73}	64	4672	988
	C_{97}	40	3880	1312
	C_{129}	32	4128	1744
	C_{161}	32	5152	2176

The 1,2-PB melts were studied for molar masses between 448 and 2176 g mol^{-1} at 453 K and at 1 atm. The selection of a higher temperature for this polymer was aimed at reducing the longer times required for attaining equilibration for these systems. All the melts were simulated with $\Delta = 0.5$. The system parameters are also reported in Table 4. To avoid system size effects associated with chain image−image interactions, for all systems studied, the root-mean-squared radius of gyration of the chains was always lower than half the box edge length.

The CPU times were calculated having as a reference a Silicon Graphics R10000 180 MHz processor. For a system of 5376 atoms of *cis*-1,4-PB the CPU time was around 1.75×10^{-2} s per attempted MC step. For a 1,2-PB melt of 5280 atoms the CPU time was about 1.67×10^{-2} s per attempted MC step. Calculated error, when reported, is estimated using the standard deviation on the results obtained once (a) a stable mean value has been reached and (b) the orientational autocorrelation function of the end-to-end distance has completely decayed to zero.

Results

Equilibration of the Melts. The usual method applied to evaluate the equilibration rate of a system is to follow the decay of the orientational autocorrelation function $\langle \mathbf{u}(t)\cdot\mathbf{u}(0)\rangle$ of a unit vector directed along the chain end-to-end vector as a function of the CPU time. Other measures of equilibration involve the mean-square displacement of the chain centers of mass and of the monomer units. Theoretically, it has been calculated[17] that the CPU time t_0 needed for the mean-square displacement of the chain centers of mass to become equal to the equilibrium mean-square end-to-end distance $\langle R^2\rangle_0$ follows the equation

$$t_0 \approx \frac{\tau}{f_{\text{EB}} p_0} \frac{n_{\text{b}}}{\bar{X}\Delta^{2.5}} \qquad (4)$$

where f_{EB} is the frequency of attempting EB moves, p_0 is the acceptance rate of the end-bridging move, τ is CPU time per MC iteration, and n_{b} is the total number of atoms in the box. This theoretical calculation predicts a linear scaling of CPU time with system size (number of atoms), expected of any MC simulation conducted at a prescribed intensive thermodynamic state point with a given mix of moves and fully confirmed by actual simulation runs. More importantly, eq 4 predicts an

Table 5. Acceptance Ratios (Percentages) of the Moves Used in the Different Systems[a]

		CB rept (25%)	rotate (10%)	CONROT (39.5%)	EB (25%)	vol fluc (0.5%)
cis-1,4-PB	C_{32}	0.70	15.0	14.5	0.29	26.9
(413 K)	C_{48}	0.50	14.5	16.0	0.30	23.4
	C_{64}	0.50	14.3	15.9	0.31	19.9
	C_{96}	0.41	14.1	15.7	0.32	16.8
	C_{128}	0.58	14.5	15.8	0.32	14.6
	C_{240}	0.43	14.2	15.6	0.32	9.5
	C_{400}	0.30	13.5	15.3	0.27	7.2
	C_{600}	0.25	13.4	15.4	0.23	5.7
	C_{1000}	0.27	13.6	15.4	0.26	4.1
1,2-PB	C_{33}	7.7	12.7	8.7	0.018	43.1
(453 K)	C_{49}	5.8	11.0	8.4	0.016	37.3
	C_{73}	4.9	10.2	7.5	0.017	30.0
	C_{97}	3.6	9.1	6.7	0.013	26.4
	C_{129}	3.2	8.6	6.1	0.014	22.5
	C_{161}	3.0	8.4	5.8	0.011	20.1

[a] The relative rates of attempting the moves are given in parentheses below the headings.

enhancement of the equilibration rate when the mean chain length and the polydispersity of the system increase. Also, it foresees an acceptance rate dependence. The acceptance percentages for the different moves in all simulated systems are reported in Table 5. It is possible that the acceptance ratio p_0 is chain length dependent and is also coupled with the acceptance rates of other moves. The synergy between EB and reptation has already been pointed out in past simulations using connectivity-altering algorithms.[17,21,20,23,24] As explained by Theodorou,[20] if the frequency of EB relative to other moves is high, it is possible that successive accepted EB moves may reverse each other, with little configurational rearrangement having occurred in between. Such "shuttling" behavior is detrimental to equilibration. Introducing a good proportion of reptation moves greatly helps in avoiding this undesirable situation, as reptation induces drastic changes in the configuration of chain ends. The shuttling problem can also be overcome by resorting to directed bridging algorithms. In systems with a bulky repeat unit, where reptation and directed bridging may have very low probabilities of acceptance, shuttling can be suppressed by combining EB and parallel tempering. Double bridging and intramolecular double rebridging, which involve exclusively internal segments and no chain ends, are also effective in eliminating shuttling. All these considerations make the equilibration rate dependent on several factors. Therefore, we can only provide qualitative comparisons of the end-bridging efficiency in equilibrating different chain length systems.

Parts a and b of Figure 4 present the evolution of $\langle \mathbf{u}(t)\cdot\mathbf{u}(0)\rangle$, with $\mathbf{u}(t)$ being the unit vector along the end-to-end vector of a chain and t the CPU time, for *cis*-1,4-PB systems of relatively short (C_{32} to C_{240}) and long chains (C_{400} to C_{1000}), respectively. In Figure 4a it can be observed that for the smaller chain system, C_{32}, the decay is slower when compared to longer chain systems (up to C_{240}), whose behavior is quite similar. This result is consistent with what has been previously observed and explained for PE end-bridging simulations:[17] The longer the chains, the more efficient EB is in decorrelating $\mathbf{u}(t)$. For chain lengths up to C_{96}, the increase of the EB efficiency is partly compensated by a decrease in efficiency (acceptance rate) of the CB reptation move. The latter is a consequence of the increase in density

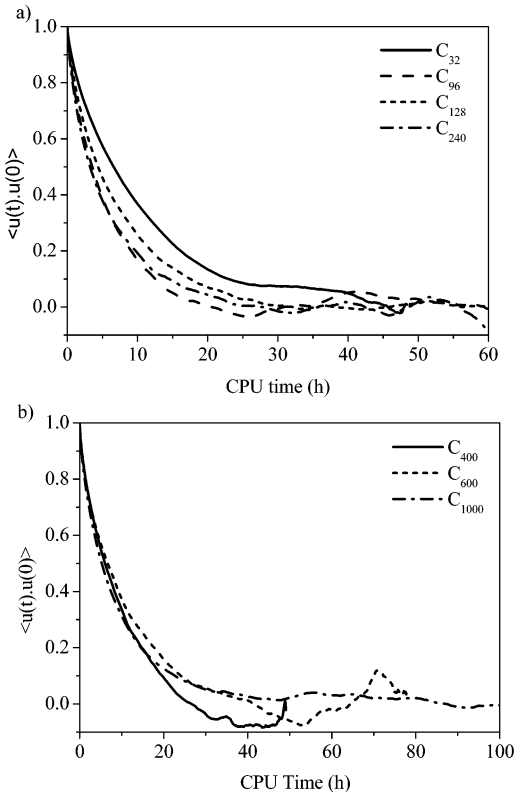

Figure 4. Decay of the chain end-to-end vector orientational autocorrelation function $\langle \mathbf{u}(t)\cdot\mathbf{u}(0)\rangle$ for (a) the C_{32}, C_{96}, C_{128}, and C_{240} *cis*-1,4-PB systems and (b) the C_{400}, C_{600}, and C_{1000} *cis*-1,4-PB systems ($T = 413$ K, $P = 1$ atm). CPU times have been corrected so that they correspond to the same number of atoms ($n = 5376$).

with chain length, which is significant for smaller molar mass systems. For the C_{128} and C_{240} melts there is an increase in the acceptance rate of CB reptation. End-bridging effectiveness improves with CB reptation acceptance by virtue of the synergy discussed above. As a result, for systems of long chains the decay of the orientation autocorrelation function will be similar to that experienced by systems of shorter chains.

Figure 4b shows the decay of $\langle \mathbf{u}(t)\cdot\mathbf{u}(0)\rangle$ for the longest chain systems (C_{400} to C_{1000}). Although the end-to-end autocorrelation function decays slightly faster for the C_{400} system, it is important to notice the similarity of the curves for systems that differ by almost a factor of 2 in the number of atoms and by more than a factor of 2 in the chain length (C_{400} vs C_{600} and C_{1000}). This result shows the good performance of the end-bridging move in equilibrating long chain systems, which has already been pointed out in the case of PE.[17]

It is interesting to compare these results with the data previously reported for *cis*-1,4-PI.[21] From the structural point of view, the only difference between *cis*-1,4-PB and *cis*-1,4-PI is the presence of pendant methyl groups in PI chains. These side groups introduce a steric hindrance, which greatly reduces the acceptance rates of the Monte Carlo moves. This decrease reaches a factor of 20 in the case of the CB reptation and the end-bridging moves. A second parameter to take into account is the number of potential neighbors of a chain end for the EB move. To preserve the chain architecture in *cis*-1,4-PI, a chain end is only allowed to bridge in one direction of the target chain. This reduces the number of potential end-bridging targets by a factor of 2 compared to the case of *cis*-1,4-PB.

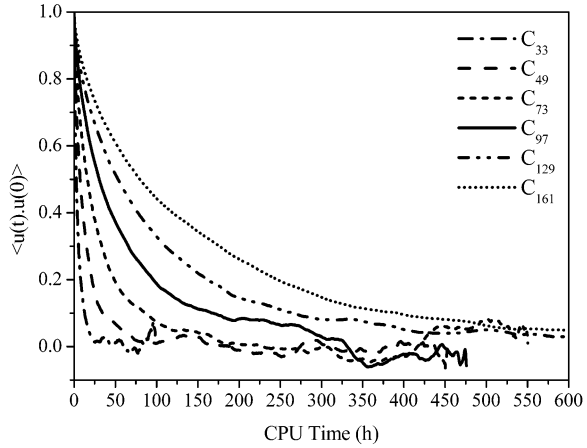

Figure 5. Decay of the chain end-to-end vector orientational autocorrelation function $\langle \mathbf{u}(t)\cdot\mathbf{u}(0)\rangle$ for the C_{33}, C_{49}, C_{73}, C_{97}, C_{129}, and C_{161} 1,2-PB systems ($T = 453$ K, $P = 1$ atm). CPU times have been corrected so that they correspond to the same number of atoms ($n = 5280$).

Figure 5 shows the orientational autocorrelation function $\langle \mathbf{u}(t)\cdot\mathbf{u}(0)\rangle$ for the different 1,2-PB melts. For all systems, the decay of the function is dependent on the chain length. That is, as the chain length increases, the decorrelation of the melts slows down. This is also confirmed by the acceptance ratios for the different Monte Carlo moves for this polymer (see Table 5). As the chain length increases, the acceptance rate for all the moves decreases steadily, especially in the case of reptation and end-bridging, which are major players in the fast large-scale equilibration of the melts. This behavior is similar to that observed previously for *cis*-1,4-PI.[21]

When comparing the results obtained for the two PB isomers, we can see that, although for very short chains (C_{32} for *cis*-1,4-PB and C_{33} for 1,2-PB) 1,2-PB decorrelates faster, as chain length increases the *cis*-1,4-PB decay is consistently faster. The slower decorrelation for 1,2-PB systems is a consequence of its bulky side groups, which prevent the acceptance of more moves due to space constraints.

The checks of equilibration presented above have been based on the decorrelation of the unit vector $\mathbf{u}(t)$ directed along the end-to-end vector of chains. The question arises whether analogous autocorrelation functions accumulated for subchains or Rouse modes, which reflect rearrangements at length scales smaller than those of the entire chain, decay with comparable efficiency. Mavrantzas et al.[17] have conducted a thorough study of orientational decorrelation of subchain vectors in polyethylene melts of chain length up to C_{500} using the end-bridging algorithm. This study showed the orientational correlation time of subchains to be an increasing function of the subchain length. On the other hand, Uhlherr et al.[18] examined the orientational decorrelation of individual skeletal bonds in a parallel directed EB-based simulation of molten C_{6000} PE, concluding that it is much slower than that of the chain end-to-end vectors! This is expected of very long chain systems, where the vast majority of bonds remain unaffected by end-bridging and reptation moves and therefore rely on concerted rotation for their orientational decorrelation. Individual bond decorrelation was found to be faster than end-to-end vector decorrelation in the 1,2-PB systems but significantly slower than end-to-end vector decorrelation in the *cis*-1,4-PB systems

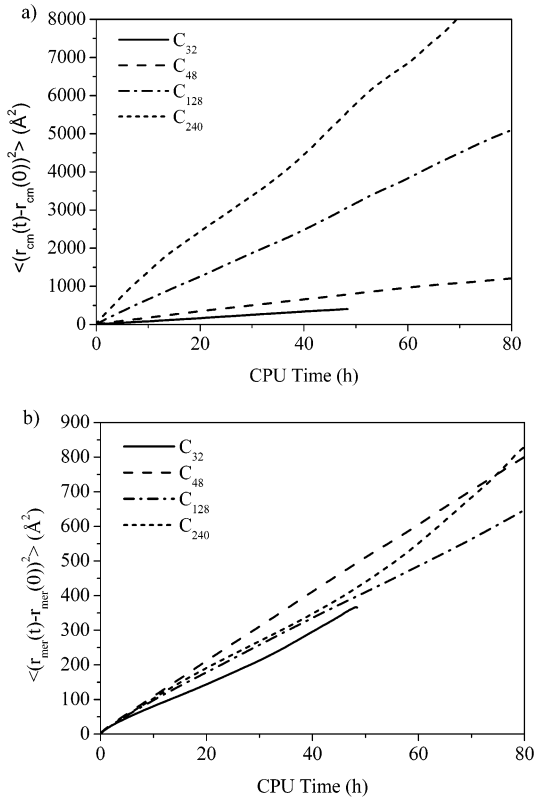

Figure 6. (a) Mean-square displacement of the chain center of mass as a function of CPU time for various *cis*-1,4-PB chain lengths ($T = 413$ K, $P = 1$ atm). (b) Mean-square displacement of the monomer center of mass as a function of CPU time for various *cis*-1,4-PB chain lengths ($T = 413$ K, $P = 1$ atm). CPU times have been corrected so that they correspond to the same number of atoms ($n = 5376$).

simulated here. In all cases the bond autocorrelation function decayed to zero by the end of the simulation; for the C_{1000} *cis*-1,4-PB system this required more than 250 CPU hours.

The ability of the end-bridging method to sample different molecular configurations is well illustrated by the mean-square displacement of the chain center of mass as a function of CPU time. Figure 6a depicts a linear increase of $\langle(\mathbf{r}_{cm}(t) - \mathbf{r}_{cm}(0))^2\rangle$ as a function of CPU time for all *cis*-1,4-PB systems, as previously observed for PE and PI. In addition, the magnitude of the displacement of the chain center of mass at a certain CPU time increases with the mean chain length. This shows how end-bridging effectively allows the long chains to diffuse faster than the short ones. An EB move introduces a huge shift of the chain center of mass for long chains, and one might argue that the displacement of the center of mass is not a reliable criterion for assessing the equilibration of the whole system. Nevertheless, it has been shown that, in conjunction with the CONROT move, the EB move can also induce a fast equilibration of the local density distribution in a melt.[17] This is quantified here by plotting the segment mean-square displacement as a function of CPU time. Figure 6b depicts the evolution of the mean-square displacement of the centers of mass of the repeat units in *cis*-1,4-PB as a function of CPU time. The shape of the curves is similar for all the melts. These results show that the larger displacement of monomers due to the CB reptation for long chains (one monomer is moved by a distance roughly equal to the end-to-end distance) is compensated for by the lower acceptance rate of CB

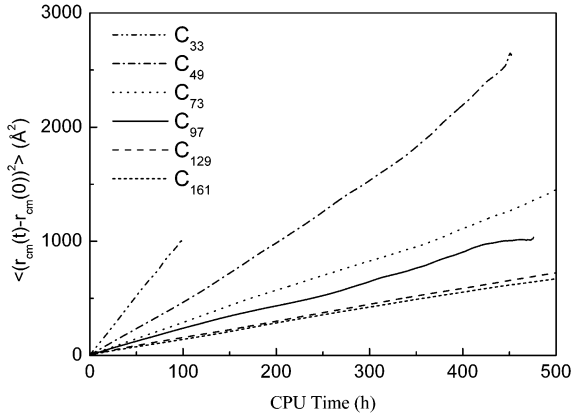

Figure 7. Mean-square displacement of the chain center of mass as a function of CPU time for various 1,2-PB chain lengths ($T = 453$ K, $P = 1$ atm). CPU times have been corrected so that they correspond to the same number of atoms ($n = 5280$).

reptation and EB moves. The C_{32} system exhibits a smaller displacement of the center of mass of monomers. This is caused mainly by the shorter end-to-end distance of C_{32} chains.

Figure 7 shows the mean-square displacement of chain centers of mass for 1,2-PB systems. Although there is a linear increase of the mean-square displacement with CPU time, as observed for *cis*-1,4-PB, here the smaller chains equilibrate faster than the longer ones. These results are consistent with the observations reported previously for the end-to-end vector autocorrelation function (Figure 5) and underline the decay in end-bridging efficiency with increasing chain length over the range of chain lengths examined for this polymer.

Conformational Properties. From atomistic Monte Carlo simulations it is possible to compute the conformational properties of the polymer chains in the melt. Usually, the accuracy of the conformations obtained through modeling is tested in terms of torsion angle distributions and chain dimension parameters, such as the end-to-end distance, radius of gyration, and characteristic ratio.[25−30] These properties can also be studied by sampling continuous unperturbed chains (CUCs). A CUC is defined as an isolated chain subject to the same potential as the melt chains, but free of nonlocal interactions.

The question of how local interactions should be defined in an atomistic model is an interesting question in itself. The usual approach is to consider as local all the bonded interactions plus the nonbonded interactions between atoms separated by up to four skeletal bonds. This approach has been introduced by Flory[25] and used in the case of PE[17] and *cis*-1,4-PI.[21] However, EB Monte Carlo simulations of PP[19,20] have shown that including interactions between atoms up to four bonds apart was not a good approximation for defining the CUCs, and longer-range nonbonded interactions should be included. To select the best approximation for CUCs, we studied four different single chain models, wherein the nonbonded interactions were active between atoms up to 4, 5, 6, and 7 bonds apart.

For each range studied, CUCs were sampled in two ways: In the first (termed "CUC without EB" in the following), single chain MC simulations were conducted subject to the CUC force field, using CONROT, reptation, and CB moves; each run provided results for a specific chain length. In the second (termed "CUC with EB" in the following) an ideal gas of chains subject only to local intramolecular interactions was simulated at melt density, using the same mix of moves as in the melt simulations; each run provided results for many chain lengths simultaneously. The single chain characteristics extracted from these two ways of simulating CUCs were identical.

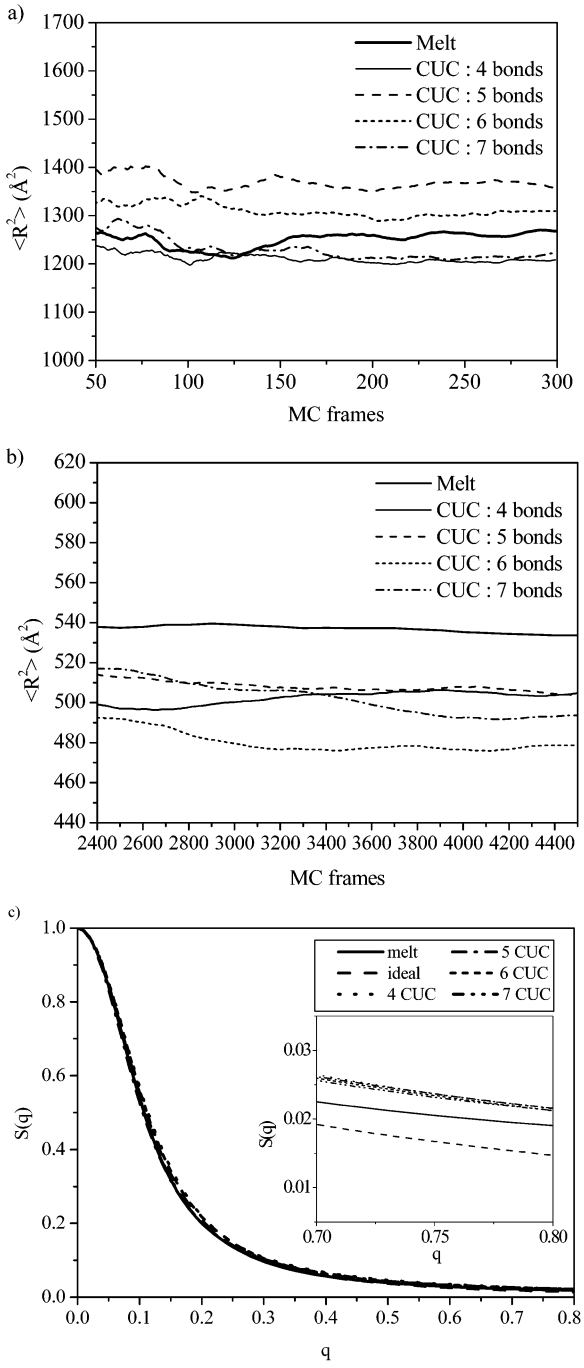

Figure 8. Mean-square end-to-end distance for melt chains and for various definitions of CUC chains in (a) C_{128} *cis*-1,4-PB at 413 K and (b) C_{97} 1,2-PB at 453 K. (c) Single chain structure factor $S(q)$ for C_{128} *cis*-1,4-PB at 413 K, as calculated from melt chains, from various CUC models and from the Debye function for an "ideal" Gaussian coil with the same mean-squared radius of gyration as the melt chains. The units of q are Å^{-1}. The high-q tail of $S(q)$ is shown magnified in the inset.

isomers. For *cis*-1,4-PB (Figure 8a) the 7-bonds and the 4-bonds CUC models give an end-to-end distance very close to that of the melt chains, whereas for 1,2-PB (Figure 8b) the 4-bonds, 5-bonds, and 7-bonds models give very comparable end-to-end distances, which are reasonably close to those of the melt chains.

Melt chains and CUCs were also compared by accumulating single chain structure factors $S(q)$ [or single chain scattering functions, $P(Q)$, in the notation of ref 30]. $S(q)$, computed as the three-dimensional isotropic Fourier transform of the reduced intramolecular pair density function $w(r)/(X - 1)$ (see structural properties below), is experimentally observable by small-angle neutron scattering from isotopically labeled chains and, by virtue of its q dependence, provides information about the chain structure at various length scales. Figure 8c displays $S(q)$ for C_{128} chains of *cis*-1,4-PB, as computed from melt chains of this specific length and for the various CUC models examined. In the same figure, labeled "ideal", is the curve for a Gaussian chain with the same mean-square radius of gyration as the melt chain, calculated from the Debye equation.[30] Similar results are obtained for other chain lengths and for 1,2-PB. Clearly, all CUC models, but also the "ideal" model, do a very good job in reproducing $S(q)$ of the melt chains. This supports the idea that the melt chains are unperturbed, to an excellent approximation. The high-q "tail" region of $S(q)$, reflecting short-range chain structure, is magnified in the inset to Figure 8c. Here one sees that the various CUC models yield very similar results, which parallel (but do not quite coincide with) the melt chain result. The ideal model is less satisfactory in this region; it does not incorporate any atomistic detail, and hence it contains no information about the intrinsic conformational stiffness of the chains.

In view of the above results we select the 4-bonds interaction to define CUCs for PB, as it is the simplest and the fastest model from the point of view of CPU time.

For *cis*-1,4-PB, the torsion angle distributions have been theoretically calculated by Mark[1] and Abe and Flory.[2] Their results predict the CH_2-CH (α) bond (see Figure 1) energy minima to be at ±120° and 0° and the CH_2-CH_2 (β) bond to prefer the trans and gauche conformational states (energy minima at $\phi = 180°$ and $\phi = \pm 60°$), with 0° defining the planar cis conformation. On the other hand, simulations by Li and Mattice[4] agreed with theoretical predictions for the β angle, whereas for the α angle they exhibit only two significant population areas around ±105° (skew) and only a very small peak at 0° (cis). These authors proposed that the disappearance of the cis conformation of the CH_2-CH bonds is due to steric repulsions of groups which are separated by the cis double bond and its two nearest methine−methylene bonds. The population distributions of the torsion angles obtained from EBMC are presented in Figure 9a (α and α′ angles, the α′ angle being symmetric to α, measured around the bond of atoms 1 and 2 in Figure 1) and Figure 9b (β angle) for the melt and the CUCs. Both melt and CUC distributions are symmetric and in very good agreement with each other. This confirms the efficiency of the EB method in equilibrating short- and long-range conformational features. For the α angle, maxima are only obtained around ±118° (skew). Therefore, the positions of the energy minima at the skew conformation are closer to those from the theoretical prediction ($\phi =$ ±120°). However, the absence of a maximum around cis agrees with the Li and Mattice simulation. For the β angle, the positions of the maxima agree with theoretical and simulation predictions.

Table 6. Trans Fractions of CH_2-CH_2 and CH_2-CH Dihedral Angles for *cis*-1,4-PB

method	CH_2-CH_2	CH_2-CH
atomistic simulation (bulk)[a]	0.400[e]	0.097[f]
atomistic simulation (single chain)[b]	0.434[e]	0.028[f]
RIS model[c]	0.368−0.333	0.048
RIS (quantum chemistry)[d]	0.40	0.13
this work	0.458[e]	0.146[f]

[a] Atomistic simulation of packed structures.[4] [b] Atomistic simulation of single chain minimized in a vacuum.[4] [c] Calculated using an empirical force field.[2] [d] Calculated using a force field based on ab initio studies.[8] [e] Trans state defined as the range from 120° to 180° and from −180° to −120°. [f] Trans state defined as the range from 150° to 180° and from −180° to −150°.

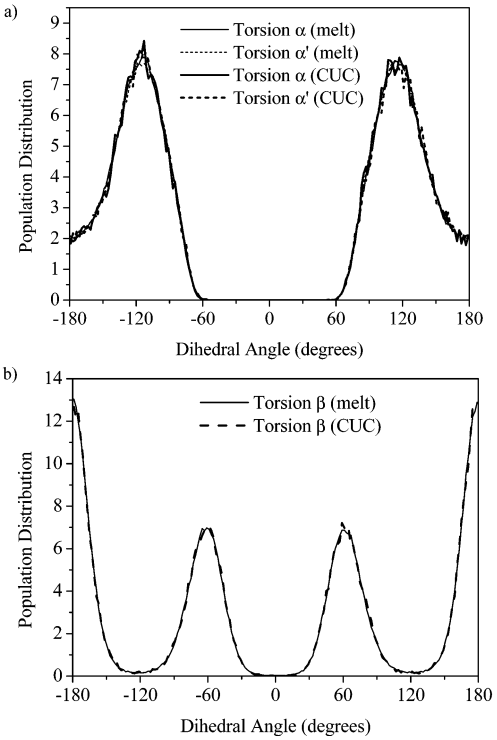

Figure 9. Distribution for *cis*-1,4-PB of (a) the two dihedral angles next to the double bond (torsion angle α and its counterpart α′ around the atom 1−atom 2 bond in Figure 1) and (b) the dihedral angle connecting two monomers (torsion angle β in Figure 1). Results from simulations of both melts and 4-bonds CUC chains are shown.

The populations of conformational states adopted by CH_2-CH_2 and CH_2-CH dihedral angles were calculated. Trans fractions for these angles are compared with literature values in Table 6. As can be seen, there is generally good agreement between the values obtained in this work and the results from other atomistic simulations and RIS model predictions.

For 1,2-PB systems, torsion angles for the melts and CUCs are plotted in Figure 10a,b. As for the other polybutadiene isomer, the angle distributions for CUC chains are very similar to those obtained from the bulk system. The torsion angles along the backbone (γ and γ' in Figure 1) are preferentially at $\phi = 180°$ and $\phi =$ ±60° (Figure 10a). These results agree with the calculations by Ma and Zhang,[3] who proposed a three-state model for this torsion angle (encompassing one trans

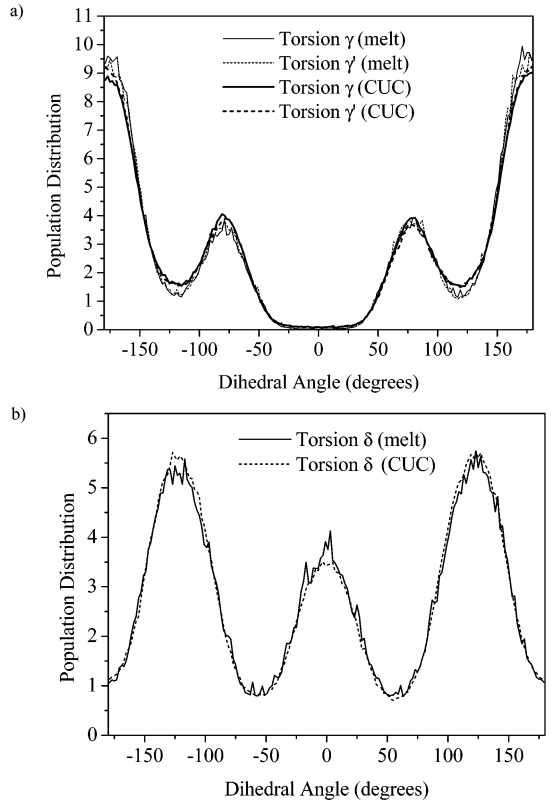

Figure 10. Distribution for 1,2-PB of (a) the two dihedral angles in the backbone (torsion angle γ and γ' in Figure 1) and (b) the dihedral angle connecting the backbone with the side group (torsion angle δ in Figure 1). Results from simulations of both melts and 4-bonds CUC chains are shown.

and two gauche conformational states) when calculating the radius of gyration using the RIS model. Figure 10b shows the distribution for the δ angle (defined in Figure 1). Maxima at cis and skew conformations ($\phi = 0°$ and $\phi = \pm 120°$) are observed. These results agree with the conformational energetics obtained for the torsions of 3-ethyl-1,5-hexadiene, used as a model for calculating 1,2-PB force field parameters.[9]

As pointed out at the beginning of the section, the calculation of the mean-squared end-to-end distance, $\langle R^2\rangle_0$, and of the mean-squared radius of gyration, $\langle R_g{}^2\rangle$, provides insight about the correctness of the configurations obtained by simulation. For *cis*-1,4-polybutadiene, $\langle R^2\rangle_0$ and $\langle R_g{}^2\rangle$ values have been calculated for melts at 413 K and are reported in Table 7. End-bridging MC allows sampling $\langle R^2\rangle_0$ and $\langle R_g{}^2\rangle$ for different chain lengths from a single simulation run. From each run, the dependence of these characteristic measures of chain size on chain length can be obtained for a range of chain lengths, from $\bar{X}(1 - \Delta)$ to $\bar{X}(1 + \Delta)$. The superposition of results from different runs, conducted for different $\bar{X}$, gives a good picture of the chain length dependence of $\langle R^2\rangle_0$. Previous works carried out using EBMC on PE[17] and *cis*-1,4-PI[21] have already shown a linear increase of the mean-squared end-to-end distance with chain length and a good prediction of this property from the CUC simulation. Figure 11a displays the increase of the mean-squared end-to-end distance in the case of the *cis*-1,4-PB melts studied here, as well as for the CUCs, for the systems up to C_{128} at 413 K. Figure 11b shows this evolution of $\langle R^2\rangle_0$ for the *cis*-1,4-PB melts for chain lengths up to C_{1000}. The results obtained with the different simulation methods are in very good agreement. A linear fit to the melt data gives the following result:

$$\langle R^2\rangle_0{}^{1/2} = 0.867M^{1/2}\,(\text{Å}) \tag{5}$$

where M is the molar mass of the chains, in g mol^{-1}. Equation 5 allows a comparison with the experimental measurements of Hadjichristidis et al.[26] for linear polybutadienes (36% cis content) under Θ conditions, based on intrinsic viscosity:

$$\langle R^2\rangle_0{}^{1/2} = 0.892M^{1/2}\,(\text{Å}) \tag{6}$$

The two results are fairly close. Differences are to be expected, as polybutadiene experimental samples contain a mix of polybutadiene repeat units. This result corroborates the efficiency of EBMC in predicting conformational properties of polymer chains.

Having computed the end-to-end distance, we can estimate the characteristic ratio C_{X-1}, defined by the following relation:

$$C_{X-1} = \frac{\langle R^2\rangle_0}{\sum_{i=1}^{X-1} l_i^{\,2}} = \frac{\langle R^2\rangle_0}{(X-1)\overline{l^2}} \tag{7}$$

where $X - 1$ is the number of links in the chain backbone and $\overline{l^2}$ is the average squared skeletal bond length. According to Abe and Flory's calculation,[2] for the 1,4-polybutadiene chain we have

$$(X-1)\overline{l^2} = \sum_i l_i^{\,2} = (1.51^2 + 1.34^2 + 1.51^2 + 1.53^2)x - 1.53^2 = 8.6967x - 2.3409\ (\text{Å}^2) \tag{8}$$

where $x = X/4$ is the number of monomer units in the chain.

Figure 12 represents the results for C_{X-1} calculated for different chain lengths as a function of the number of carbons in the chains. C_∞ is calculated by extrapolating the linear fit to intersect the C_{X-1} axis at infinite chain length. The value obtained for C_∞ is 4.7, which is in good agreement with the experimental result of 4.9 $\pm$ 0.2 obtained by Moraglio[27] and Abe and Fujita[28] and with the value of 5.1 reported by Hadjichristidis[26] from Θ solution measurements.

Table 8 reports the mean-squared end-to-end distance $\langle R^2\rangle_0$ and the mean-squared radius of gyration $\langle R_g{}^2\rangle$ for 1,2-PB melts. Comparing results for both parameters, it can be observed that for all systems $\langle R^2\rangle_0 \cong 6\langle R_g{}^2\rangle$, as expected of random coils. This is confirmed by the fact that $\langle R^2\rangle_0$ values for melts and CUCs are in accord, within the simulation uncertainty. The values of end-to-end distance vs chain length are plotted in Figure 13. It can be seen that, as for the other polybutadiene isomer, the behavior is linear for the melts as well as for the CUC systems, although the latter present slightly higher dispersion because the runs were shorter. Results can be fit to the equation

$$\langle R^2\rangle_0 = 0.419M\ (\text{Å}^2) \tag{9}$$

with M being the molecular weight, in g mol^{-1}. This

Table 7. Mean-Squared End-to-End Distance and Mean-Squared Radius of Gyration for *cis*-1,4-PB Melts and CUC at 413 K and 1 atm

	C_{32}	C_{48}	C_{64}	C_{96}	C_{128}	C_{240}	C_{400}	C_{600}	C_{1000}
					Melt				
$\langle R^2\rangle_0$ (Å^2)	284 ± 13	447 ± 21	617 ± 55	953 ± 119	1320 ± 152	2542 ± 256	3745 ± 307	6156 ± 974	9841 ± 1231
$\langle R_g^2\rangle$ (Å^2)	42 ± 1	69 ± 1	93 ± 1	142 ± 2	211 ± 2	436 ± 3	586 ± 33	1071 ± 27	1507 ± 59
					CUC				
$\langle R^2\rangle_0$ (Å^2)	268 ± 13	426 ± 37	589 ± 58	924 ± 100	1168 ± 174				
$\langle R_g^2\rangle$ (Å^2)	51 ± 1	65 ± 1	92 ± 1	142 ± 3	179 ± 3				

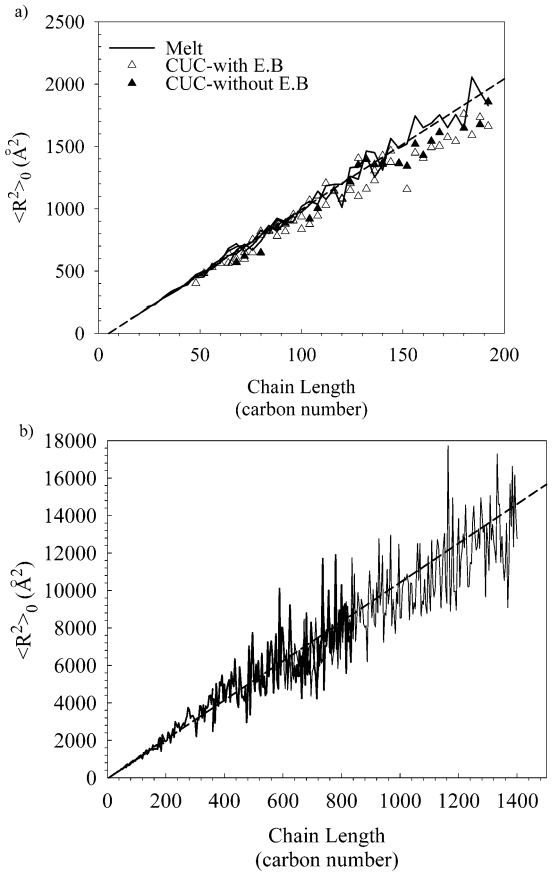

Figure 11. *cis*-1,4-PB chain mean-square end-to-end distance as a function of chain length (a) for systems up to C_{128}. CUC chain results computed with and without end-bridging are also shown. The dashed line represents the linear fit to the melt data. (b) Same as (a) for melt systems up to C_{1000}.

implies the following molecular weight dependence for the radius of gyration:

$$\langle R_g^2\rangle^{1/2} = 0.264M^{1/2}\,(\text{Å}) \qquad (10)$$

Hattam et al.[29] report chain dimensions for 1,2-PB near Θ conditions from intrinsic viscosity measurements. They obtained $\langle R^2\rangle_0 = 0.608M$ at 339 K with a temperature coefficient of $\mathrm{d}\ln\langle R^2\rangle_0/\mathrm{d}T = -1.7 \times 10^{-3}$ K^{-1} between 289 and 339 K. Using this temperature coefficient to extrapolate to our simulation temperature of 453 K gives $\langle R^2\rangle_0 = 0.501M$ (Å^2), which is higher than the predicted value by ca. 20%. This difference is mainly due to the fact that our 1,2-PB simulations employed considerably lower molecular weights than the measurements (please see discussion of characteristic ratios below). On the other hand, on the basis of RIS model calculations at 340 K, Ma and Zhang[3] report

$$\langle R_g^2\rangle^{1/2} = 0.298M^{1/2}\,(\text{Å}) \qquad (11)$$

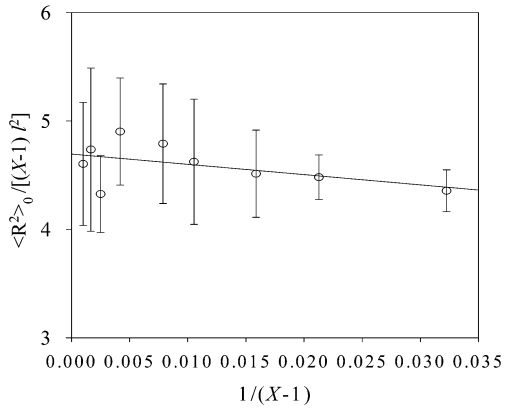

Figure 12. Characteristic ratio for *cis*-1,4-PB systems calculated for the systems simulated as a function of the inverse number of bonds in a chain. The line is a linear fit to the data.

When corrected with the experimental temperature coefficient, this gives $\langle R_g^2\rangle^{1/2} = 0.270M^{1/2}$ (Å), which is by only 2% higher than our simulation estimate, eq 10. The theoretical calculations of Ma and Zhang were conducted for isotactic 1,2-PB, whereas an atactic polymer was simulated here. Isotactic chains typically experience stronger conformational constraints, leading to an increase in chain dimensions. Thus, one would expect our values to be somewhat lower than those of Ma and Zhang.

Using an expression similar to eq 7, it is possible to calculate the dependence of the characteristic ratio on chain length. In this case, the number of skeletal bonds in the denominator is $(X - 1)/2$ and $(\overline{l^2})^{1/2} = l = 1.53$ Å. Results for $C_{(X-1)/2}$ as a function of the inverse number of skeletal bonds are plotted in Figure 14. It can be seen that, despite the limited data, a linear fit can be applied. The use of the linear fit is justified, as the characteristic ratio is known to become linear in the inverse chain length at sufficiently large chain lengths (ref 30, p 129). From the extrapolation to infinite chain length a value of 5.4 is obtained for C_∞. Extracting a characteristic ratio from the relation $\langle R^2\rangle_0 = 0.501M$ (Å^2), based on the data of Hattam et al.[29] after application of their temperature correction, leads to $C_\infty = 5.8$. This is by 7% higher than our predicted value for long chains.

In light of the above comparisons with Hattam et al.'s[29] experimental data and Ma and Zhang's[3] RIS calculations, we conclude that our simulation predictions for the stiffness of 1,2-PB chains are in reasonable agreement with literature values.

Thermodynamic Properties. The specific volume (v) can be predicted from the constant-pressure simulations carried out in this work as a result of the implementation of the volume fluctuation move. The values of specific volume for *cis*-1,4-PB obtained at atmospheric pressure for the different chain lengths and temperatures are plotted in Figure 15. The general behavior is in good agreement with that expected of a

Table 8. Mean-Squared End-to-End Distances and Mean-Squared Radius of Gyration for 1,2-PB Melts and CUC at 453 K and 1 atm

	C_{33}	C_{49}	C_{73}	C_{97}	C_{129}	C_{161}
			Melt			
$\langle R^2\rangle_0$ (Å^2)	144 ± 6	233 ± 16	388 ± 27	574 ± 80	736 ± 79	930 ± 121
$\langle R_g^2\rangle$ (Å^2)	23 ± 1	38 ± 1	63 ± 1	91 ± 1	119 ± 3	161 ± 9
			CUC			
$\langle R^2\rangle_0$ (Å^2)	135 ± 5	232 ± 14	366 ± 30	501 ± 46	672 ± 69	915 ± 93
$\langle R_g^2\rangle$ (Å^2)	23 ± 1	38 ± 1	64 ± 1	87 ± 1	122 ± 1	166 ± 7

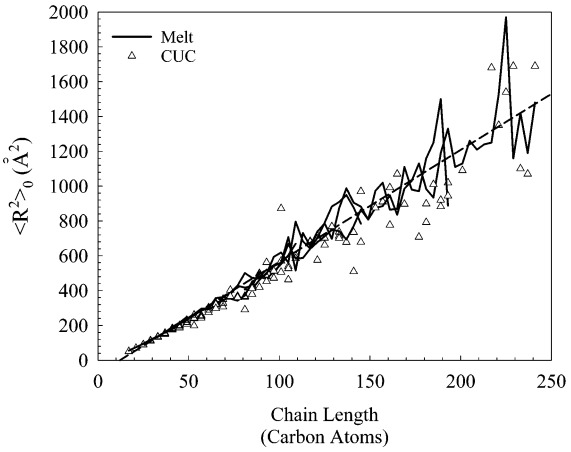

Figure 13. 1,2-PB chain mean-square end-to-end distance as a function of chain length. Results for CUC chains computed without end-bridging are also shown. The dashed line represents the linear fit to the melt data.

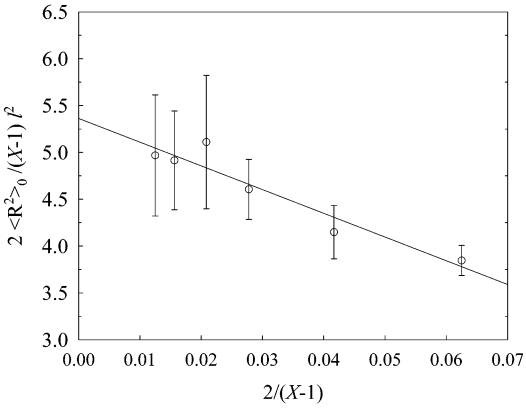

Figure 14. Characteristic ratio for 1,2-PB calculated for the systems simulated as a function of the inverse number of carbon atoms in a chain. The line is a linear fit to the data.

polymer melt. The specific volume decreases with temperature. Furthermore, v decreases monotonically with increasing chain length in a hyperbolic fashion, until it reaches a practically constant value for very long molecules. It can be observed in the figure that v does not change significantly for chains longer than 200 carbons. The evolution of v with the mean chain length $\bar{X}$ is usually described in the literature by a relation of the form

$$v = v_\infty + \frac{v_0}{\bar{X}} \tag{12}$$

where v_∞ is the specific volume for at infinite chain length and v_0 describes the rate at which v decreases. Fitting the data calculated at 413 K according to eq 12 gives the following values: $v_0 = 3.344$ cm^3 g^{-1} and $v_\infty = 1.148$ cm^3 g^{-1}. Figure 16 shows the comparison of our

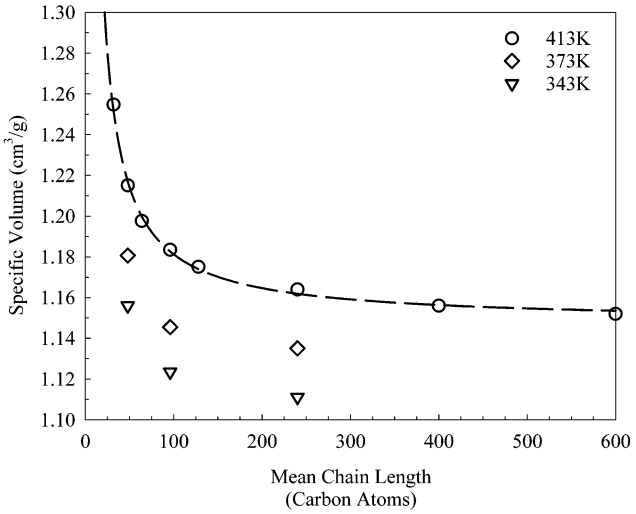

Figure 15. Mean chain length dependence of the specific volume v for *cis*-1,4-PB systems simulated at 343, 373, and 413 K ($P = 1$ atm). The dashed line corresponds to a hyperbolic fit according to eq 12.

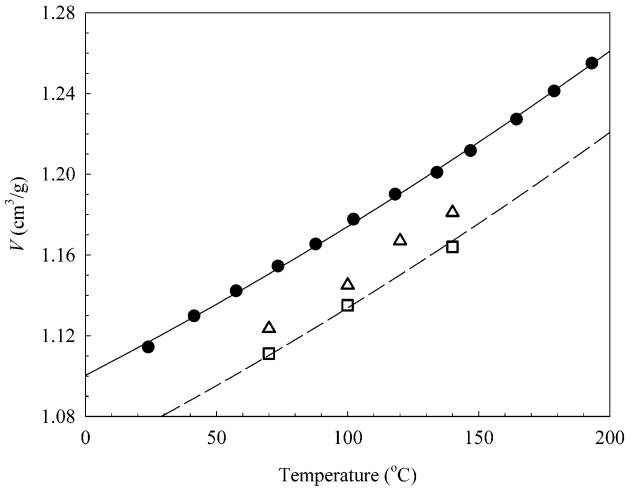

Figure 16. Temperature dependence of the specific volume v for the simulated *cis*-1,4-PB systems C_{96} (open triangles) and C_{240} (open squares). Filled circles are the experimental data obtained by Yi and Zoller (ref 31). Dashed and solid lines correspond to fits according to eq 13.

results with the experimental values measured by Yi and Zoller,[31] who used the Tait equation of state to fit the data. According to the Tait equation, as fitted to experimental data, the temperature dependence of v at 0 atm for a 1,4-polybutadiene (40% of *cis*-1,4-PB) is described by the following equation:

$$v(t) = 1.1004 + 6.718 \times 10^{-4}t + 6.584 \times 10^{-7}t^2 \quad \text{cm}^3\,\text{g}^{-1} \tag{13}$$

with t being the temperature, measured in °C.

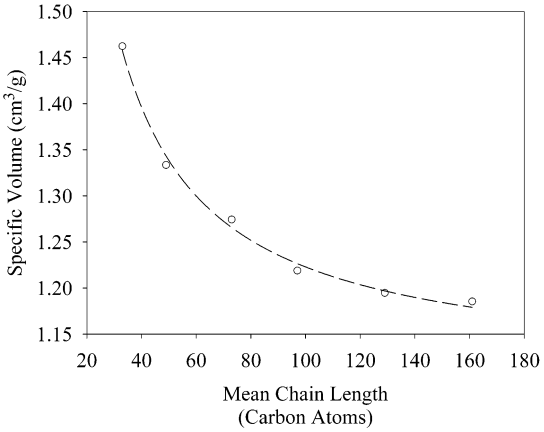

Figure 17. Mean chain length dependence of the specific volume v for 1,2-PB systems simulated at 453 K ($P = 1$ atm). The dashed line corresponds to a hyperbolic fit according to eq 12.

The simulation data exhibit a comparable behavior to that of the experimental values. In fact, it is possible to fit our results with the same first- and second-order coefficients; only the constant term $v(0)$ of the equation differs: the C_{240} values can be fitted with $v(0) = 1.06$ cm^3 g^{-1}. Clearly, the simulation underestimates the specific volume; simulated long-chain *cis*-1,4-PB melts are by about 3.7% denser than the real material. A comparison with the work of Fetters et al.[32] confirms the underestimation of the specific volume. These experiments, carried out on polybutadiene (50/40/10 trans/cis/vinyl) at 413 K, gave $v = 1.211$ cm^3 g^{-1}. The difference between this experimental value and our simulation is 5%. A small part of this offset is due to the fact that a melt consisting of a mix of repeat units should be less dense than the pure *cis*-1,4-PB.[32] The main reason for our underestimation of the specific volume, however, is our use of a constant bond angle model. Constraining the bond angles during the simulation deprives the model of the "free volume" that would be generated through fast vibrations of the atoms. A reparametrization of the model (increased atomic radii) would be required to capture this effect within our fixed bond angle representation.

Specific volume values obtained for 1,2-PB melts are plotted in Figure 17. As in the case of *cis*-1,4-PB, as the number of repeat units increases, v decreases. Nevertheless, the maximum chain length studied here is insufficient for v to reach a constant value. The data were fitted using eq 12, obtaining the values $v_0 = 11.57$ cm^3 g^{-1} and $v_\infty = 1.107$ cm^3 g^{-1}. On the other hand, the specific volume obtained from the Tait equation[31] for 1,2-PB (8/5/87 trans/cis/vinyl) at the same $P-T$ conditions is $v_\infty = 1.2447$ cm^3 g^{-1}. The greater disparity between v_∞ values obtained from fitting simulated and experimental data than in the case of *cis*-1,4-PB is largely due to the limited range of chain lengths that have been simulated for 1,2-PB. Already from Figure 17 one can see that the specific volume tends to level off for large chain lengths at a value higher than expected from the hyperbolic fit of eq 12 to the available simulation data. Simulations of higher molecular weight 1,2-PB melts would be required to capture v_∞ for 1,2-PB reliably.

Under the same conditions of temperature, pressure, and molecular weight, the simulations predict almost identical volumes for *cis*-1,4-PB and 1,2-PB. For C_{160} melts at 453 K and 1 atm, extrapolation of the simulation data for *cis*-1,4-PB leads to $v = 1.198$ cm^3 g^{-1}. The corresponding simulation value for 1,2-PB is 1.188 cm^3 g^{-1}. On the other hand, for large molecular weights at 453 K and 1 atm, the Tait equation fitted to experiment gives $v = 1.2427$ cm^3 g^{-1} for (50/40/10 trans/cis/vinyl) and 1.2447 cm^3 g^{-1} for (8/5/87 trans−cis-vinyl) PB. In view of these results, the *relative* volumetric behavior predicted by the simulations is reasonable. For both *cis*-1,4-PB and 1,2-PB the density is overestimated in relation to experiment. The overestimation seems to be somewhat stronger in the case of 1,2-PB.

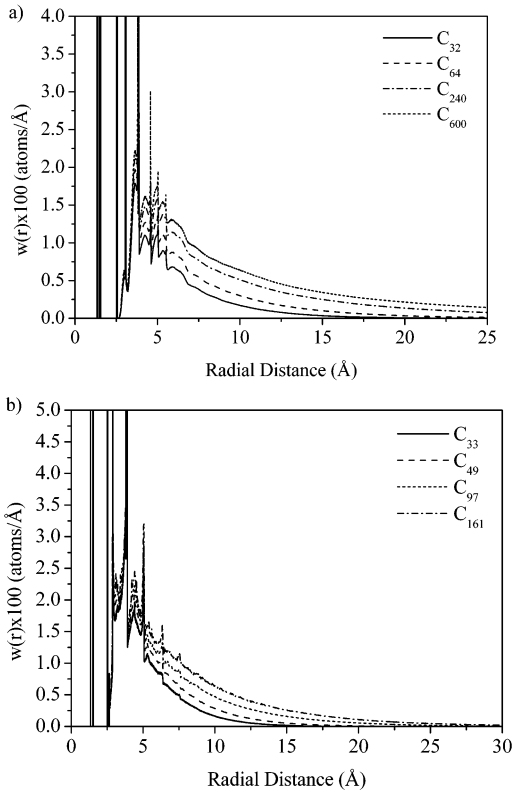

Figure 18. Intrachain pair density function $w(r)$ for (a) various *cis*-1,4-PB systems at 413 K and 1 atm and (b) several 1,2-PB systems at 453 K and 1 atm.

Structural Properties. Structural properties can be evaluated by calculating the intrachain pair density function $w(r)$ and the intermolecular pair distribution function $g(r)$. Not only do these functions provide a measure of conformation and packing in the amorphous bulk but, recently, the study of their shape has been proposed as a fast and easy tool for evaluating the miscibility behavior of binary polymer blends.[33]

The intrachain pair density function reflects correlations along a single chain. Parts a and b of Figure 18 depict $w(r)$ for different *cis*-1,4-PB systems (C_{32}, C_{64}, C_{240}, and C_{600}) and for a representative set of 1,2-PB melts (C_{33}, C_{49}, C_{97}, and C_{161}), respectively. The first Dirac peaks (at 1.35, 1.51, and 1.53 Å) correspond to pair interactions between atoms connected by one bond. These peaks are also seen in the results of Okada and Furuya[34] from molecular dynamics simulations of a single *cis*-1,4-PB molecule of 200 repeat units. The next peak, at 2.54 Å, is due to carbon pairs separated by two bonds. The other peaks at distances greater than 3 Å reflect the conformational preferences of the chains. For example, for the *cis*-1,4-PB, the peak at 3.07 Å is due to atom pairs separated by three bonds. In the case of

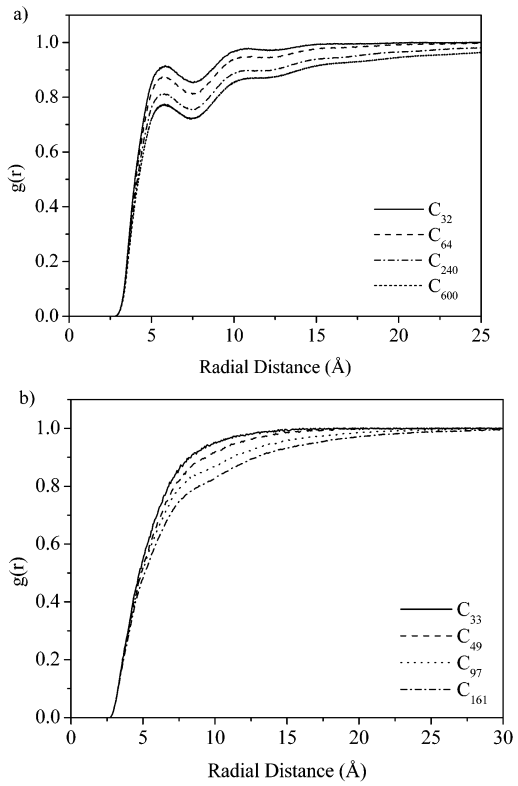

Figure 19. Intermolecular pair distribution function $g(r)$ for (a) various *cis*-1,4-PB systems at 453 K and 1 atm and (b) several 1,2-PB systems at 453 K and 1 atm.

1,2-PB, the peak at 5.04 Å is due to two atoms separated by four bonds, but also to two atoms 4 (Figure 1) belonging to two connected mers. The positions of these sharp peaks are chain length independent. The longer range part of $w(r)$ depends on the chain length and so reflects the intrinsic density of the chain segment cloud. The longer the chains, the higher the density of segments one expects to find around a reference segment. As previously reported for *cis*-1,4-PB,[4,34] no peaks are observed for distances longer than 7 Å, where $w(r)$ falls as a smooth curve.

Complementary information on the structure of the PB melts can be obtained from the intermolecular pair distribution function $g(r)$. Parts a and b of Figure 19 display this function for different chain lengths for *cis*-1,4-PB and 1,2-PB, respectively. As for PE and PI melts, the $g(r)$ function for PB isomers exhibits the so-called "correlation hole effect".[35,36] That is, at short distances, $g(r)$ is suppressed because the segment cloud of the chain prevents segments of other chains from approaching the reference segment. For *cis*-1,4-PB, the peak around 5.8 Å reflects the average position of the first intermolecular neighbors. This position of first neighbors is shorter than in the case of PI (around 6.2 Å), reflecting the absence of methyl substituents. A small shift of the first peak in $g(r)$ toward small distances is observed as the mean chain length increases. This shift mirrors the density increase with chain length, already shown in Figure 15. In the case of 1,2-PB, especially for the shorter chain melts (C_{33} and C_{49}), the intermolecular pair distribution function appears remarkably structureless. It rises monotonically to unity. The various types of carbon atoms in the polymer arrange themselves in such a way as to display no significant amount of overall liquid structure beyond the hard-core repulsion, which appears around 2.70 Å. As the length of the chains increases, shoulder peaks appear at 8.4 and 13.5 Å, simultaneously with a decrease in the height of the $g(r)$ curves. This emergence of some structure is related to the increase of density, which makes the packing tighter. That the peaks are less distinct and appear at longer distances than for other polymers (PE, *cis*-1,4-PI and *cis*-1,4-PB) implies that 1,2-PB is less structured. That is, the chains are less packed, probably due to the presence of the bulky side group, which takes up a substantial fraction of the size of the repeat unit.

Maranas et al.[33] proposed that there is a correlation between the shape of the intermolecular pair distribution function of pure polymers and the regularity of mixing in binary polymer blends. Pairs of polymers with a tendency toward immiscibility present similar $g(r)$ shapes, whereas pairs of polymers with different intermolecular pair distribution functions are stabilized as one phase upon mixing. Using this approach, it is possible, at this point, to gain insight about the miscibility of PB isomers and *cis*-1,4-PI.[21] In order to proceed, the shape of the $g(r)$ should be catalogued as structured, unstructured, or intermediate, depending on the number and relative height of the peaks. By the above discussion, the intermolecular pair distribution function of 1,2-PB has been classified as unstructured going to intermediate (as chain length increases), while *cis*-1,4-PI[21] and *cis*-1,4-PB have been categorized as structured. We evaluate the expected mixing behavior from the similarity or disparity of the shapes for each pair. In *cis*-1,4-PB/1,2-PB and *cis*-1,4-PI/1,2-PB blends, the two components have different $g(r)$ shapes, which should promote regular mixing. On the other hand, *cis*-1,4-PB/*cis*-1,4-PI blends should be destabilized as a consequence of their similar $g(r)$ shapes. These results reflect the experimental trends quite well. For blends of 1,2-PB miscibility has been established both with PI (miscible in all ratios)[37−40] and with 1,4-PB.[41] In the case of *cis*-1,4-PB/*cis*-1,4-PI systems, there is abundant experimental work reporting partial miscibility with a LCST-type phase diagram.[42−44]

Although this analysis offers an easy and rapid indication of the miscibility tendency for polybutadiene and polyisoprene blends, it also has serious limitations. First, it is obvious that the classification of the pair distribution functions is of utmost importance. The models provided in the article by Maranas et al.[33] do not reflect the variety of $g(r)$ shapes encountered in all polymers, so a clear-cut classification may be difficult. Moreover, the pair distribution function, and therefore its classification, can be strongly dependent on factors such as the chain length, as observed for 1,2-PB systems. Finally, the evaluation of $g(r)$ shapes is unable to predict complex miscibility behaviors or the degree of partial miscibility.

Conclusions

Melts of two polybutadiene isomers, *cis*-1,4-PB and 1,2-PB, have been simulated using atomistic Monte Carlo with fixed bond length and bond angle models. The capability of the end-bridging MC algorithm to equilibrate long chain systems (up to 1000 atoms for *cis*-1,4-PB, and 161 carbons for 1,2-PB) has been established. We have shown that this method is especially powerful in the case of large model systems of *cis*-1,4-PB.

In general, the simulation results for the conformational properties of the melts agree very well with

experimental data, demonstrating the ability of the algorithm to equilibrate the studied systems fully at all length scales and of the force field to reproduce the physical properties of the polybutadienes. Specific volumes are underpredicted, mainly because of the use of constant bond angles in the simulations. Agreement with experiment tends to be better in the case of *cis*-1,4-PB melts than for 1,2-PB systems, noticeably in the case of specific volume. Several reasons can explain this difference. First, the maximum mean chain length studied for 1,2-PB (C_{161}) is only one-sixth of the longest chains simulated for *cis*-1,4-PB (C_{1000}), making extrapolations to infinite chain length less reliable for 1,2-PB. Second, although the same force field is used for both polybutadienes, 1,2-PB has a large side group, for which nonbonded interactions are difficult to parametrize. Finally, it is important to point out that experimental data for pure polybutadiene isomers are very scarce. Therefore, comparisons are necessarily made against polybutadienes of different microstructure and discrepancies are attributable, to some extent, to the presence of other repeat units.

The analysis proposed by Maranas et al.[33] for correlating pure component $g(r)$ shapes to miscibility behavior was attempted for polybutadiene/polyisoprene and *cis*-1,4-polybutadiene/1,2-polybutadiene binary blends. The results agree with the experimental evidence, reinforcing the connection between the pure component properties of polymers and their mixing behavior, as stated by Maranas et al.[33] Nonetheless, the simplicity of the approach prevents making distinctions between full and partial immiscibility. A more detailed study of *cis*-1,4-PB/*cis*-1,4-PI blends using atomistic end-bridging MC is currently underway.[45]

Acknowledgment. This work was supported by the European Commission through the NEWRUP Network, funded through the Training and Mobility of Researchers program of the European Commission (Contract ERB-FMRX-CT98-0176). P. Gestoso also acknowledges the support of a Marie Curie Host Development fellowship to ICE/HT-FORTH from the European Commission (Contract HPMD-CT-2000-00054).

References and Notes

(1) Mark, J. E. *J. Am. Chem. Soc.* **1966**, *88*, 4354.
(2) Abe, Y.; Flory, P. J. *Macromolecules* **1971**, *4*, 219.
(3) Ma, H.; Zhang, L. *Polym. J.* **1994**, *26*, 121.
(4) Li, Y.; Mattice, W. L. *Macromolecules* **1992**, *25*, 4942.
(5) Kim, E.; Misra, S.; Mattice, W. L. *Macromolecules* **1993**, *26*, 3424.
(6) Misra, S.; Mattice, W. L. *Macromolecules* **1993**, *26*, 7274.
(7) Gee, R. H.; Boyd, R. H. *J. Chem. Phys.* **1994**, *101*, 8028.
(8) Smith, G. D.; Paul, W. *J. Phys. Chem. A* **1998**, *102*, 1200.
(9) Smith, G. D.; Paul, W.; Monkenbusch, M.; Willner, L.; Richter, D.; Qiu, X. H.; Ediger, M. D. *Macromolecules* **1999**, *32*, 8857.
(10) de Pablo, J. J.; Laso, M.; Suter, U. W. *J. Chem. Phys.* **1992**, *96*, 2395.
(11) Siepmann, J. I.; Frenkel, D. *Mol. Phys.* **1992**, *75*, 59.
(12) Leontidis, E.; de Pablo, J. J.; Laso, M.; Suter, U. W. *Adv. Polym. Sci.* **1994**, *116*, 283.
(13) Leontidis, E.; Forrest, B. M.; Widmann, A. H.; Suter, U. W. *J. Chem. Soc., Faraday Trans.* **1995**, *91*, 2355.
(14) Frenkel, D.; Smit, B. *Understanding Molecular Simulation*; Academic Press: New York, 1996.
(15) Dodd, L. R.; Boone, T. D.; Theodorou, D. N. *Mol. Phys.* **1993**, *78*, 961.
(16) Pant, P. V. K.; Theodorou, D. N. *Macromolecules* **1995**, *28*, 7224.
(17) Mavrantzas, V. G.; Boone, T. D.; Zervopoulou, E.; Theodorou, D. N. *Macromolecules* **1999**, *32*, 5072.
(18) Uhlherr, A.; Doxastakis, M.; Mavrantzas, V. G.; Theodorou, D. N.; Leak, S. J.; Adam, N. E.; Nyberg, P. E. *Europhys. Lett.* **2002**, *57*, 506. Uhlherr, A.; Leak, S. J.; Adam, N. E.; Nyberg, P. E.; Doxastakis, M.; Mavrantzas, V. G.; Theodorou, D. N. *Comput. Phys. Comm.* **2002**, *144*, 1.
(19) Samara, C. T. Simulation of polypropylene of various tacticities with the Monte Carlo method. Ph.D. Thesis, University of Patras, Patras, Greece, 2000.
(20) Theodorou, D. N. In Nielaba, P., Mareschal, M., Ciccotti, G., Eds. *Bridging Time Scales: Molecular Simulations for the Next Decade*; Springer-Verlag: Berlin, 2003; pp 67−127.
(21) Doxastakis, M.; Mavrantzas, V. G.; Theodorou, D. N. *J. Chem. Phys.* **2001**, *115*, 11339.
(22) Theodorou, D. N.; Suter, U. W. *Macromolecules* **1985**, *18*, 1206.
(23) Uhlherr, A.; Mavrantzas, V. G.; Doxastakis, M.; Theodorou, D. N. *Macromolecules* **2001**, *34*, 8554.
(24) Karayiannis, N. Ch.; Giannousaki, A. E.; Mavrantzas, V. G.; Theodorou, D. N. *J. Chem. Phys.* **2002**, *117*, 5465.
(25) Flory, P. J. *Statistical Mechanics of Chain Molecules*; Wiley-Interscience: New York, 1969.
(26) Hadjichristidis, N.; Zhongde, X.; Fetters, L. J.; Roovers, J. *J. Polym. Sci., Polym. Phys.* **1982**, *20*, 743.
(27) Moraglio, G. *Eur. Polym. J.* **1965**, *1*, 103.
(28) Abe, M.; Fujita, H. *J. Phys. Chem.* **1965**, *69*, 3263.
(29) Hattam, P.; Gauntlett, S.; Mays, J. W.; Hadjichristidis, N.; Young, R. N.; Fetters, L. J. *Macromolecules* **1991**, *24*, 6199.
(30) Mattice, W. L.; Suter, U. W. *Conformational Theory of Large Molecules*; Wiley: New York, 1994.
(31) Yi, Y. X.; Zoller, P. *J. Polym. Sci., Part B: Polym. Phys.* **1993**, *31*, 779.
(32) Fetters, L. J.; Lohse, D. J.; Richter, D.; Witten, T. A.; Zirkel, A. *Macromolecules* **1994**, *27*, 4639.
(33) Maranas, J. K.; Kumar, S. K.; Debenedetti, P. G.; Graessley, W. W.; Mondello, M.; Grest, G. S. *Macromolecules* **1998**, *31*, 6988.
(34) Okada, O.; Furuya, H. *Polymer* **2002**, *43*, 971.
(35) de Gennes, P. G. *Scaling Concepts in Polymer Physics*; Cornell University Press: Ithaca, NY, 1979; pp 62−68.
(36) Schweizer, K. S.; Curro J. G. *Adv. Polym. Sci.* **1994**, *116*, 319.
(37) Roland, C. M. *Macromolecules* **1987**, *20*, 2557.
(38) Roovers, J.; Toporowski, P. M. *Macromolecules* **1992**, *25*, 3454.
(39) Miller, J. B.; McGrath, K. J.; Roland, C. M.; Trask, C. A.; Garroway, A. N. *Macromolecules* **1990**, *23*, 4543.
(40) Trask, C. A.; Roland, C. M. *Macromolecules* **1989**, *22*, 256.
(41) Sakurai, S.; Hasegawa, H.; Hashimoto, T.; Hargis, I. G.; Aggarwal, S. L.; Han, C. C. *Macromolecules* **1990**, *23*, 451.
(42) Trask, C. A.; Roland, C. M. *Polym. Commun.* **1988**, *29*, 332.
(43) Sakurai, S.; Jinnai, H.; Hasegawa, H.; Hashimoto, T.; Han, C. C. *Macromolecules* **1991**, *24*, 4839.
(44) Hasegawa, H.; Sakurai, S.; Takenaka, M.; Hashimoto, T.; Han, C. C. *Macromolecules* **1991**, *24*, 1813.
(45) Gestoso, P.; Nicol, E.; Theodorou, D. N., manuscript in preparation.

MA034033L